Determining the Rydberg constant using X-ray Diffraction

Andrew D. Miller
Imperial College, London
adm114@ic.ac.uk | CID: 00929697
Laboratory Partner: Ian M. Yeung

January 16, 2017

Abstract

Utilising the characteristics of x-ray radiation, the internal structure of certain materials can be investigated using various techniques. A LD Didactic X-ray Apparatus was used in combination with a selection of radiation sources and detectors to investigate the properties of metals and compounds using two basic theories: Moseley's Law and Bragg's diffraction law. A series of experiments were conducted to determine the theory's validity, and the value of the Rydberg constant was determined to be $(10.32 \pm 0.71) \times 10^6 m^{-1}$.

I. Introduction

X-rays were an area of science with extreme interest in both the last part of the 19th Century and beginning of the 20th. In 1895, Wilhelm Röntgen discovered x-rays but it wasn't until 1912 when Max von Laue observed X-ray diffraction in crystals that they were considered a form of electromagnetic radiation [1]. In the same year, William Lawrence Bragg discovered that different elements produced characteristic x-ray lines when bombarded with electrons, and developed his law that relates the scattering angles of x-rays with evenly-spaced crystalline planes of reflection [2]. In the years that followed, physicist Henry Moseley carried out a systematic study of these characteristic lines, following a conversation with Niels Bohr, who was a pioneer of the atomic model (see Figure 1). Moseley discovered that although the individual optical spectra of atoms were complicated, the x-ray spectra progressed in a very simple fashion. He then published his law that explained this trend, where he related his work very strongly to that of Bohr's [3]. This work was very important to the development of quantum theory, since both Bohr's own formula for atomic spectra and Moseley's law for x-ray spectra were used in the quantum formulation of atoms.

From this explosion of investigation, there emerged many areas of x-ray experimentation. Two of the main ones are spectroscopy and crystallography, which is used to investigate aspects of crystalline material structure, including atomic arrangement, crystallite size, and imperfections present. These techniques use Bragg's diffraction law to analyse the characteristic K_α and K_β lines, as well as the "braking radiation" present to determine the nature of the sample. An example of modern-day x-ray analysis can be found in a paper by K. Norrish [5], where x-ray fluorescence has been used to categorise a large number of geological samples.

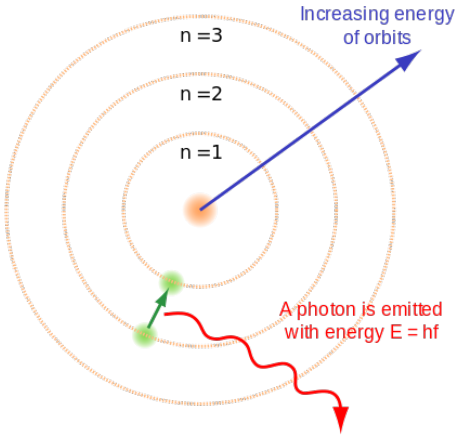

Figure 1: *A simplified schematic of the Bohr model of the atom. This consists of atoms with energy levels that increase in energy further from the nucleus [4].*

II. Theory

X-ray radiation from a source consists of two main components: "braking radiation" and characteristic x-rays. The positions of the characteristic x-rays with

respect to angle are governed by Bragg's law, which is a special case of Laue diffraction and gives the condition on the diffraction angle (θ) for complete constructive interference to occur:

$$n\lambda = 2d\sin\theta \tag{1}$$

where λ is the wavelength of the incoming radiation, d, in this case, is the inter-atomic spacing of the lattice layers, and n is a positive integer (full derivation of this condition is in the appendix). The inter-atomic lattice spacing can be converted to the lattice constant (dubbed a_0) of a crystal, since for cubic crystal unit cell, such as NaCl, the following relation holds: $2d = a_0$.

The other aspect of characteristic x-rays that is of interest is their energy. Originally Bohr's model yielded the Rydberg formula for hydrogenic atoms (i.e. alkali metals):

$$E = R_\infty\left(\frac{1}{n_f^2} - \frac{1}{n_i^2}\right)Z^2 \tag{2}$$

where R_∞ is the Rydberg constant (with the value of $1.0973 \times 10^7 m^{-1}$ [6]), Z is the atomic number of the element, and $n_{i,f}$ are the principal quantum numbers of the initial and final states (full derivation of this condition is in the appendix). However, this does not take into account the fact that the nuclear charge (Ze) of an atom is partially screened by inner electrons. So when an electron in the K-shell absorbs an x-ray and gets ejected, on average, only the charge $(Z - \sigma_k)e$ acts on the electron during this ionisation.This gives rise to Moseley's law:

$$E = h\nu = B(Z - \sigma_k)^2 \tag{3}$$

where B is a constant of the order of the Rydberg energy, and σ_k is known as the screening coefficient, which is constant for sufficiently large Z ($>\approx 30$). This equation can be rewritten in terms of absorption edges, which is "the energy at which there is a sharp rise (discontinuity) in the (linear) absorption coefficient of X-rays by an element, which occurs when the energy of the photon corresponds to the energy of a shell of the atom" [7]. Thus, in terms of the energies for the K-shell transitions:

$$\frac{1}{\sqrt{\lambda_k}} = \sqrt{R_\infty}(Z - \sigma_k) \tag{4}$$

where $\sqrt{\lambda_k}$ is the wavelength at which the K-absorption edge occurs. Thus in plotting a graph of $\sqrt{\lambda_k}$ against Z, the values of both the Rydberg constant and the screening coefficient (σ_k) can be determined.

III. Methods

The main instrument that was used throughout the experiments was a Leybold® X-Ray Apparatus device. This contained all major elements of the investigation: the x-ray source, detector, and sample table, all while being able to send the detector's output to the computer interface for analysis.

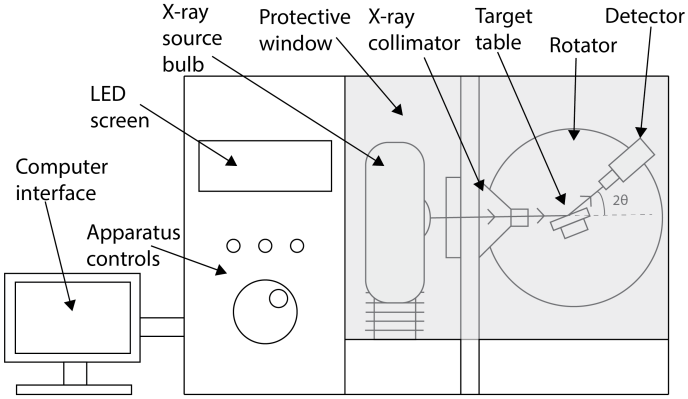

Figure 2: *A basic schematic of the X-ray Apparatus. This is shown to be in the Bragg configuration as this ensures that the angle between detector and incident x-ray path was twice that between target and incident x-ray path.*

The interface software was installed on a MacBook Pro[1], so that the transfer of data between systems was not required and such that the analysis could take place immediately. The x-ray source used for the experiments was a Molybdenum target, as it has a good all-round performance as an x-ray source, since "it has short wavelength, high energy x-rays and an appreciable bremsstrahlung spectrum" [8]. In addition to this, a Copper target was used to compare properties of x-ray sources, but since a suitable spectrum could not be obtained, in the end this source was not used for this experiment. However according to theory, the Copper target would have produced a spectrum more suitable for Bragg reflection experiments, due to the low amount of bremsstrahlung and clearer characteristic peaks.

i. Setup for investigating Bragg's Law

A useful aspect of this apparatus was that it could be configured to move just the target, just the detector, or even both together in the Bragg configuration (see Figure 2 for details). For this configuration to work correctly, the setup had to be calibrated: the rotating sample table such that the maximum intensity signal was detected, and the detector to prevent a "zero"

[1] This was my personal computer

error. The first stage was completed with a small amount of manual adjustment of the table by a few fractions of a degree. The second part was covered by the scanning range, since all scans started below 0^o then the x-ray source has to pass through the *true* zero point (see Figure 3).

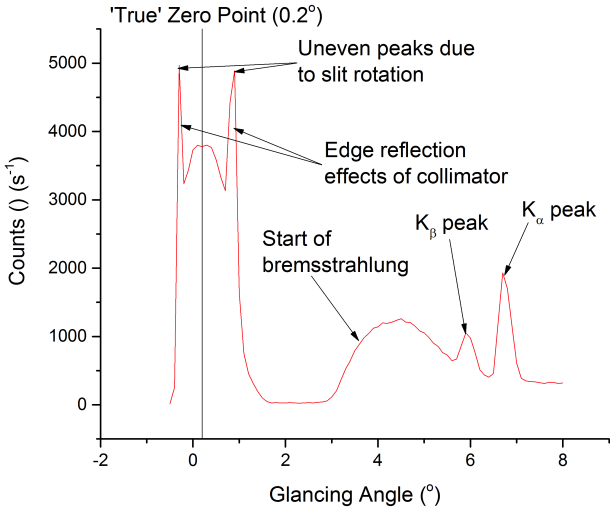

Figure 3: *Graph showing the basic features of an x-ray spectrum, including bremsstrahlung continuum, zero error correction, and features of the collimator.*

The x-crystal sample was scanned with the source in this Bragg configuration from -0.5^o to 41^o in 0.1^o intervals for 10 seconds each.

ii. Setup for investigating Moseley's Law

In order to determine the K-absorption edges necessary, the apparatus was used in conjunction with several metal attenuators, in the form of caps, which could be fitted on both the x-ray collimator and the detector. These are tabulated in Table 1 with various data about each element in the attenuator:

Table 1: *Metal Attenuators and Corresponding Data*

Element	Symbol	Atomic Number (Z)
Zirconium	Zr	40
Molybdenum	Mo	42
Silver	Ag	47
Indium	In	49
Copper	Cu	29
Iron	Fe	26
Nickel	Ni	28

In order to prove that both the position of the attenuator in the setup and the time for each measurement had no effect on the results, three scans with each metal cap was completed: firstly covering the x-ray source, secondly covering the detector, and finally for a longer period of time (15 seconds for each measurement). Once the attenuated measurements had been taken, the transmission curve of each attenuator was calculated through the relation:

$$T = \frac{I}{I_0} \tag{5}$$

where T is the transmission, I is the intensity with attenuation, and I_0 is the intensity without attenuation. From the transmission curve, the K-absorption edge of each attenuator was determined by X-ray Apparatus and thus a graph representing Equation 4 can be plotted.

IV. Data & Results

i. Investigating Bragg's Diffraction Law

Figure 4 shows the basic x-ray spectrum of an NaCl crystal taken with the X-ray Apparatus in the Bragg configuration.

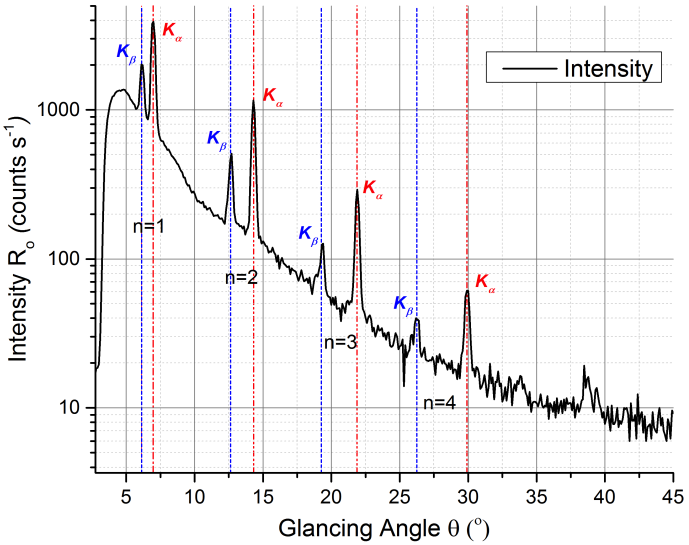

Figure 4: *Graph showing how intensity of reflected x-rays changes with angle. Notice both the overall bremsstrahlung continuum as well as four clear diffraction orders of characteristic x-ray peaks (possibly five).*

The overall sloping trend of the graph appears as a continuum and represents "braking radiation". This is produced by the deceleration of charged particles when deflected by other charged particles, releasing a photon in order to satisfy the conservation of energy. Several sharply defined lines on a spectrum are observed, which correspond to characteristic K_α and K_β

transitions when the source is bombarded with high energy electrons. Figure 2 shows the angles that the characteristic x-ray peaks occur at:

Table 2: *Characteristic X-ray peaks for K_α and K_β transitions in sodium chloride (NaCl) crystal*

Order	Mean Angle / ^{o}	Total Error / ^{o}
1 (K_α)	6.13333	0.06973
2 (K_α)	12.62	0.04328
3 (K_α)	19.28	0.04274
4 (K_α)	26.25667	0.08183
1 (K_β)	6.95	0.07682
2 (K_β)	14.29	0.04519
3 (K_β)	21.87667	0.02177
4 (K_β)	29.92333	0.04885

ii. Determining the Lattice Constant of NaCl

The literature value of λ_{K_α} and λ_{K_β} as $63.095pm$ and $71.08pm$ respectively [8], and upon rearranging Bragg's law the value of the lattice constant (a_0) can be determined by plotting a graph of, such as Figure 5 and calculating the gradient:

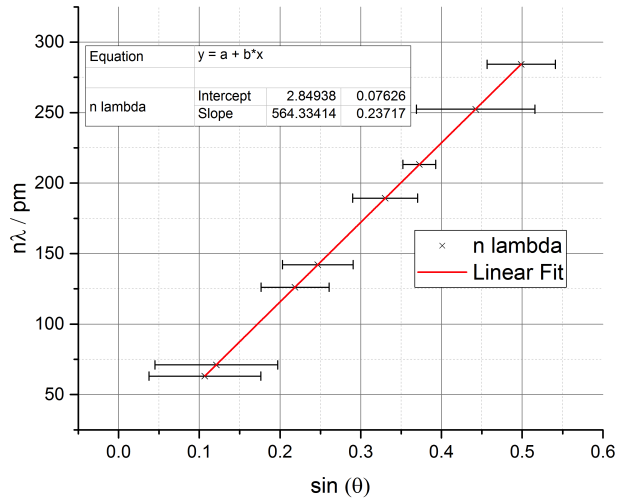

Figure 5: *Graph of wavelength against angle. Theory suggests that the y-intercept should be fixed at zero, so two values of the lattice constant were determined.*

So when the y-intercept is not fixed, the lattice constant is $564.33 \pm 0.24pm$, and with a fixed intercept, a_0 is $572.38 \pm 1.41pm$ - this is extremely close to the literature value of $564.0pm$.

iii. Metal Attenuation

One key aspect of placing a material in the path of a radiation source is to observe how much radiation passes through it, and this is calculated as an transmission coefficient or attenuation coefficient, given by Equation 6. Table 3 below shows the various coefficients for each of the seven filters used:

Table 3: *Attenuation coefficient for metal attenuators*

Filter	K_β attenuation (%)	K_α attenuation (%)
Zr*	6.97	48.53
Mo	15.57	12.76
Ag	1.93	0.61
In	10.21	7.24
Cu	9.68	6.18
Fe	0.01	0.14
Ni	46.17	47.80

These results show that all metals except Zirconium attenuate K_α and K_β peaks at approximately the same amount. However adding Zr in front of the x-ray source acts as a 'band-filter' that filters out the fK_β transition line but not the K_α one.

There is also an added effect from the Beer-Lambert law [9] that contributes to the value of the attenuator's transmission, but for the purposes of this investigation its effects can be ignored.

iv. Determining Rydberg's constant

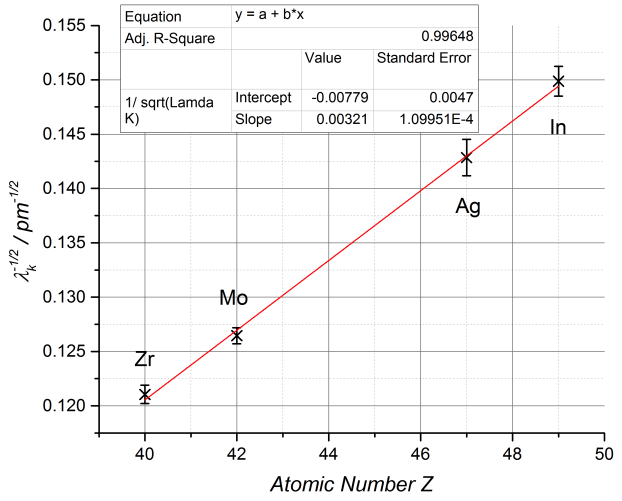

Figure 6: *Graph of $\sqrt{\lambda_k}$ against Z. Note that there are only 4 metal filters here that can be used under the assumptions stated earlier.*

Having determined the transmission curves of the metals, the values of the K-absorptions edges were

calculated in terms of wavelength, and were plotted against atomic number (see Figure 6).

The graph has a relatively good fit, with an adjusted R^2 value very close to 1, thus justifying the relationship stated in Equation 4. The Rydberg constant was determined to have the value $(10.32 \pm 0.71) \times 10^6 m^{-1}$, which is very close to the literature value. The screening coefficient, which for moderately heavy nuclei is constant, was assessed to be 2.427 ± 2.773 - this measurement has an extremely large uncertainty overall.

V. Uncertainties & Discussion

The first part of the investigation, involving Bragg's law and the Lattice constant were relatively simple, and yielded an accurate value for a_0 and a low uncertainty. In hindsight if the experiment were to be repeated, there would be more than one reading taken of the un-attenuated crystal spectrum, so there is plenty of data to compare. The main contribution to error in the lattice constant was the determination of the peak maximum, and corresponding angle. This experiment could have been taken further with investigation into more detail of the crystalline structure, such as determining the Miller indices of the mono-crystal and comparing that to a powder sample of NaCl (see equation below):

$$d = \frac{a_0}{\sqrt{h^2 + k^2 + l^2}} \tag{6}$$

where h, k, l are the Miller indices. In terms of the attenuation experiment, it was clear that the attenuation of K_α and K_β peaks in spectra by metals was not perfectly equal (see Table 3). This could be due to a number of reasons, including possible impurities in the metal foils, deformities in its surface, or even over-exposure and saturation of x-rays. This could be improved by completing this part for a larger variety of metals, particularly those that could acts as 'band-filters' that remove one of the two characteristic peaks.

In terms of determining Rydberg's constant, there are many errors to discuss and the first of these are the zero errors that occurred in the measurements. When the metal foil caps were placed on the detector or collimator, there was an additional shift that was required to line up the K_α and K_β peaks of 0.2^o. Another aspect to mention is the fact that only four of the seven metal filters could be used to determine R_∞, since Ni, Cu and Fe all had atomic numbers less than 30, which is outside the scope of Moseley's law and the screening coefficient become non-linear. Thus, if we compare the literature values of λ_k for these three metals to the results, there is no obvious jump that occurs at that point (see Figure 7)

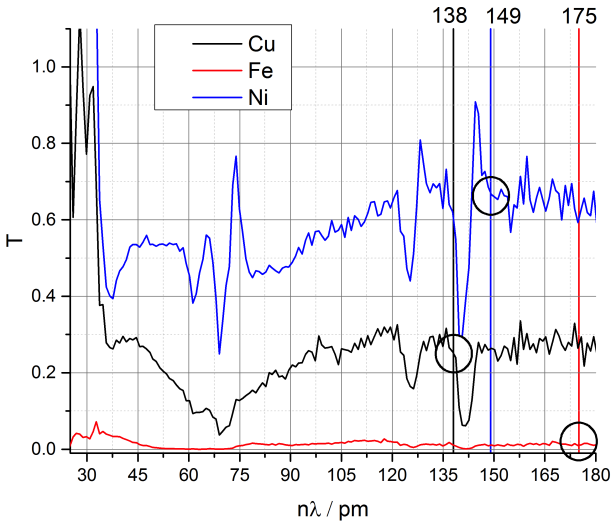

Figure 7: *Graph showing part of the transmission curves of copper, iron and nickel. Notice that there is not an absorption edge at the predicted values (circles on graph)*

By comparing gradients for the four heavier metals, it was found that as a metal gets heavier, the further the value of λ_k moves from the absorption edge (this effect was observed only slightly in graphical form - see appendix). Thus it has been postulated that the K-absorption edge will shift its location from the expected position on the spectrum, which is what we observed in Figure 7. One final aspect to investigate is the uncertainty in the screening coefficient (σ_k). Its value can be calculated from the y-intercept, but requires that the gradient of the line be known as well:

$$\sigma_k = -\frac{b}{\sqrt{R_\infty}} \tag{7}$$

where b is the y-intercept of the straight line and $\sqrt{R_\infty}$ is the square-rooted Rydberg constant, which is also the gradient of the line. So when the individual errors are added in quadrature, the biggest contribution to σ_k's uncertainty is from the gradient itself. This was tested when each error was reduced by a factor of ten to see the largest contribution, and it was found that the value changed the most when the gradient's uncertainty was reduced.

VI. Conclusions & Future Development

In conclusion, it has been shown that x-rays emitted from a source can be used to investigate multiple areas of physics: not only the structure of the sample crystal they are directed towards, but also the emissions of

characteristic x-rays can allow other properties of metals to be measured. It has been shown that Bragg's law of diffraction can be utilised to calculate an internal constant of a crystalline compound, and that metals can attenuate x-rays. This can be harnessed to determine the Rydberg constant through Moseley's Law, and since the associated error is extremely good (approximately 2% of the calculated value).

In terms of improving the errors themselves, this can be split into the random and systematic errors of the investigation. Reducing the random errors can be accomplished by using more *independent* trials, as well as additional sets of repeat readings. This is because in allowing the detectors, samples and x-ray sources to be switched off and not used between each trial, or alternatively one could wait for a longer period of time between sets of readings, a more accurate variance may be observed in the measurements. For the systematic error, simply taking more data points (e.g. by using a smaller angle interval) and extending our observations further into the high and low angle points means that there is much more information to reduce the systematic error.

There are many areas for further exploration within this experiment as well, and a major one is getting more attenuators to investigate the trend of decreasing nuclear charge so that the transition from a linear equation to a non-linear one can be seen. Other possible investigations include using x-ray fluorescence to verify Moseley's law, comparing various different crystal types (including powder), and also using different x-ray sources.

Word Count (checked in Word): 3054

References

[1] Friedrich, W; Knipping, P; von Laue, M. (1912). *Interferenz-Erscheinungen bei Röntgenstrahlen*. Sitzungsberichte der Mathematisch-Physikalischen Classe der Königlich-Bayerischen Akademie der Wissenschaften zu München 303.

[2] Bragg, W.H. (1913). *The reflection of x-rays by crystals*. Nature Issue 2280: 467-477. (Nature Publishing Group).

[3] Moseley, H.G.J. (1913). *The high-frequency spectra of the elements*. Philosophical Magazine Series 6: 1024?1034.

[4] Obtained from `http://www.universetoday.com/46886/bohrs-atomic-model/`

[5] Norrish, K; Hutton, J.T. (1969). *An accurate X-ray spectrographic method for the analsysi of a wide range of geological samples*. Geochimica et Cosmochimica Acta, Volume 33, Issue 4: 431-453

[6] The NIST Reference for Constants, Units and Uncertainties (2014). Obtained at `http://physics.nist.gov/cgi-bin/cuu/Value?ryd`

[7] Online Dictionary of Crystallography (2016). Obtained from `http://reference.iucr.org/dictionary/Absorption_edge`

[8] McGinty, J. (2016). *X-Ray Diffraction B2*. Imperial College London

[9] IUPAC. (1997). *Compendium of Chemical Terminology*. 2nd ed. (the "Gold Book")

VII. Appendices